Electrospun Polystyrene/PANI-Ag fibers for organic dye removal and antibacterial application

Electrospun Polystyrene/PANI-Ag fibers for organic dye removal and antibacterial application

Jolly Bhadra[a], Hemalatha Parangusan[a], Anton Popelka[a], Marian Lehocky[b,c], Petr Humpolicek[b,c], Noora Al-Thani[a,*]

[a]*Centre for Advanced Materials (CAM), Qatar University, P.O. Box 2713 Doha, Qatar,*

[b]*Centre of Polymer Systems, Tomas Bata University in Zlin, Trida Tomase Bati 5678, 76001 Zlin, Czech Republic*

[c]*Faculty of Technology, Tomas Bata University in Zlin, Vavreckova 275, 76001 Zlin, Czech Republic*

[*]*Corresponding author E-mail address: n.al-thani@qu.edu.qa (N. Al-Thani).*

ABSTRACT

Herein we report superior dye-degradation performance for polyaniline-silver (PANI-Ag) nanoparticle coated on polystyrene (PS) electrospun membrane by in situ-polymerization method. Morphological study of the coated membrane shows PANI-Ag nanofibril network with average diameter of 100 nm around micrometer diameter electrospun PS fiber. X-ray diffractogram (XRD) showed the formation of PANI-Ag nanocomposite and according to Bragg's reflection the crystal diffraction plans are from the FCC structure of Ag. Thermal analysis of the composite reveals glass transition temperature observed in the temperature range from 100-110°C for both PANI and PANI-Ag coated samples and 5 % residue is left after heating it to 800 °C, which may be due to presence of Ag in the composite. Antimicrobial study indicates that pure PANI sample do not exhibit any antibacterial performance for both Staphylococcus aureus and Escherichia coli. However, antibacterial behavior is observed for PANI-Ag samples when experiment is performed. The photocatalytic degradation of AZG dye solution using PS/PANI-Ag membrane shows 85 % of AZG dye degraded within 180 min. The stability check of the nanocomposites is done by FTIR analysis PS/PANI-Ag nanocomposite is not affected and no chemical transformation takes place during the photodegradation process.

Keywords: Photocatalysis, polyaniline, dye degradation, electrospun nanofibers, antimicrobial

1. Introduction

Different types of organic dyes have been utilized in many industries such as textile industries, leather tanning industries, food technology, paper production, agricultural research, photo electrochemical cells and hair dyeing [**1-7**]. A large amount of water is used by leather industry in the dyeing steps producing dye-containing effluents [**4**]. Draining untreated dye containing effluents and coloured wastewater generated by various industries are unsafe to the water bodies, because it will harm the life of aquatic organism [**8**]. Most of the dyes has high solubility in aqueous medium and high toxicity, which can cause severe damage to the environment and living beings.

There are many popular methods to treat coloured wastewater such as, microbiological method, adsorption, chemical oxidation, membrane filtration and photocatalysis processes [**9-14**]. One of most studied method in this field is microbiological methods [**15**]. However, this method is not effective to

most of dyes because they are mostly chemically stable and resistant to microbiological attack. Other conventional methods such as adsorption, membrane filtration are not very effective because of high solubility of the synthetic dyes. More recently advanced oxidation process has became more popular due to some additional advantages. This process leads the generation of sufficient quantities of hydroxyl radicals to oxidize most of the complex chemicals those are present in the water effluent [**16,17**].

Photocatalysis is a type of advanced oxidation process leads to conversion of hazardous complexes to innocuous products [**18**]. This process can be utilized to clean a wide variety of dangerous compounds in different wastewater sources. Different photocatalyst have been used in the field of photodegradation. It has some drawbacks including fast recombination of charge carriers and difficulties in the separation from water. In order to solve this problem, variety of methods have been developed. One of the interesting approach is to develop flexible fibrous membranes. The electrospun nanofibers are synthesized and reported by few researchers. The incorporation of ZnO in polyimide fibers has been reported by Ding et al., and it has efficient degradation ability toward organic dyes [**19**]. At the same time, the conditions, reaction time, and chemical requirements for the photocatalytic process are very optimal [**20**]. The most important requirement for any photocatalytic reaction to take place is the presence of catalytically active species. When a light of certain wavelength incident on surface of the photocatalytic material the electrons get excited and hop from the valance band to the conduction band, leaving behind with holes in the valence band with energy equivalent to the band gap energy of the irradiated light. These electrons and the holes undertake oxidation and reduction reactions with the organic pollutants [**21**] and degrade these organic compounds into simpler harmless form.

Among different types of catalytically active materials conductive polymer material, polyaniline (PANI) has extensively explored in the catalytic and photocatalytic area [**22-24**]. PANI is a n-conjugate long-chain polymer and upon doping it shows very high conductivity. A PANI-ZnO composite with quasi-shell — core structure is prepared by coating a PANI layer on the surface of ZnO. They reported that the PANI coating can significantly enhance the photocatalytic property of ZnO and inhibit the photocorrosion of ZnO. Another research group prepared PANI/Ag/Ag_3PO_4 composites showing very strong photocatalytic capability [**25**]. The introduction of PANI in the PANI/Ag/Ag_3PO_4 composite has significantly increase both the photocatalytic degradation performance and the photocatalytic degradation stability of Ag_3PO_4. However, using different forms of nanocomposites for the wastewater treatment by using photocataclytic technique has a problem of removing the powder composites after treating the wastewater.

In this work, PANI-Ag fiber-like structured nanocomposites prepared by insitu chemical oxidation method and deposited on the surface of electrospun PS membrane. Subsequently, the characterization, antimicrobial analysis and photocatalytic degradation of Azocarmine G dye (AZG) using PANI-Ag coated PS electrospun membrane is studied systematically.

2. Material and Methods

2.1. Material

Aniline ($C_6H_2NH_2$, MW = 93.13, 99.5 %), N,N-dimethylformamide (DMF) (linear formula $HCON(CH_3)_2$, > 99.8 %, molecular weight (MW): 73.09 g/mol, d=∼0.944g/ml (lit.)), polystyrene (linear formula

[$CH_2CH(C_6H_5)$] n, average MW: —280.000 g/mol, Tg = 100 °C, d = 1.047 g/ml at 25 °C), and silver nitrate ($AgNO_3$) from Sigma Aldrich. Hydrochloric acid 37 % (HCL, MW: 36.46, d = 1.18g/cm^3 (20 °C)), ammonium peroxodisulphate (APS) ($(NH_4)\ 2S_2O_8$, MW: 228.2 g/mol, d = 1.98 g/cm^3 (20 °C)), are purchased VWR Chemicals Analwr Normapur. All the chemicals are used without further treatment.

2.2. Preparation of electrospinning PS membrane

For electrospinning at room temperature, PS solution is prepared by dissolving the polymer at 20 % w/v in DMF. The solution is placed in an oil bath under constant stirring at 60 °C for 24 h prior to electrospinning. After that, the solution is loaded in 10 ml syringe with a stainless-steel needle with an inner diameter of 0.23 mm. Electrospinning is performed using a setup with a horizontal rotating drum configuration inorder to get fiber uniform diameter. The working conditions are as follows: a 15 cm distance from the needle to the collector, a flux of 1.5 ml/h provided by a syringe pump, and a voltage of 15 KV applied to the needle to yield nanofibers. The fibers are collected after 6 h of electrospinning on an aluminum foil covering rotating collector. The electrospinning membrane is sandwiched between two pieces of aluminum foil and then pressed using a weight of 250 g for 24 h at room temperature to make the PS membrane stable and easy to handle.

2.3. Preparation of PANI coated PS membrane

Chemical polymerization method is used to coat PANI on PS membrane using HCL as dopant. In this process, aniline is added to 1 M aqueous HCL solution under constant shaking. Pre-prepared PS membranes are added to the aniline — HCl solution. The oxidant solution is prepared using ammonium persulphate with water and 1 M HCl is added dropwise to the aniline over a period of 30 min. The whole reaction condition is maintained for 24 h at constant shaking in ice bath maintaining temperature of 5 °C, and pH 4. The solution turns green, indicating the formation of PANI. The PS membranes are removed from the polymerized solution and washed several times with distilled and dried in room temperature for 24 h before use.

2.4. Preparation of PANI-Ag coated PS membrane

The preparation of PANI-Ag composite is done by two steps process. At the first step, $AgNO_3$ is reduced to Ag nanoparticles by irradiation UV-vis light of wavelength 390 nm. Followed by chemical polymerization of aniline monomer in the presence of Ag nanoparticles using the same method as mentioned in section **2.2**.

2.5. Characterization techniques

Scanning electron microscopy (SEM) is used to study the surface morphology of the electrospun PS nanofibres, as well as the grain size of all the samples (NanoSEM Nova 450). A Fourier-transform infrared spectrometer (FTIR) (8101 M, Shimadzu) is used to the study the chemical interaction between the polymers. To study the thermal properties of the PANI, thermogravimetric analysis (TGA) and differential scanning calorimetry (DSC) are performed using a Perkin Elmer Pyris thermogravimetric analyser and Perkin Elmer Precisely Jade differential scanning calorimeter, respectively.

2.5.1. Photocatalytic aktivity

The photocatalytic activity of as-prepared PS/PANI-Ag membrane is investigated by the decolorization of aqueous solution of Azocarmine G dye as model pollutant. The reaction is carried out under UV light using a UV-lamp (390 nm). In a typical experiment, required amount (5 mg) of membranes are immersed in 2 mg/l of AZG dye solution. Before irradiation, the dye solution was kept under dark condition for 30 min to ensure complete adsorption of the dye. Then the solution is exposed to the UV irradiation. During the photodegradation process, the solutions are collected every 60 min and analyzed by UV-vis spectrophotometer. The degradation efficiency of the AZG dye is estimated by the following equation,

$$\text{Photodegradation efficiency (\%)} = \frac{C_0 - C_t}{C_0} \text{ X } 100$$

Where C_0 is the initial concentration of AZG dye and C_t is the final concentration of AZG dye solution at different time intervals.

2.5.2. Antimicrobial aktivity

The antibacterial properties were evaluated for both PANI and PANI AG samples by means of Minimum inhibitory concentration (MIC) -determined by the CLD / EUCAST macrodilution method. Samples were shredded in a frit to fine powder to ensure a good homogeneity of the prepared suspension prior to the test. From both samples, stock concentrated suspensions were prepared in Mueller-Hinton Broth (MHB) sterile medium and further diluted to a concentration of 16; 8; 4; 2; 1; 0.5; 0.25; 0.125; 0.06 and 0.03 mg / ml. To each concentration the same amount of bacterial suspension (inoculum) in MHB was added and after thorough homogenization the tubes were incubated for 24 h at 35 °C. Then 0.1 ml was withdrawn from each tube and spread on the surface of the agar (always in duplicate for each concentration). After incubation at 35 °C for 18 — 24 hours, the growth of test bacteria on the surface of the plates was evaluated and a minimum inhibitory concentration was determined accordingly. Tests were performed with Staphylococcus aureus CCM 4516 (inoculum concentration 1.8 x 106 cfu / ml) and Escherichia coli CCM 4517 (inoculum concentration 0.5 x 106 cfu / ml).

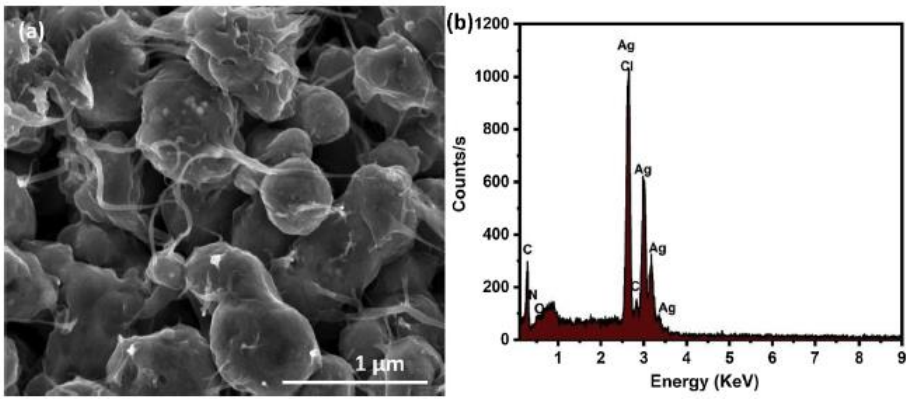

Fig. 1. FESEM images of (a) PANI-Ag composite, (b) EDX spectra for PANI-Ag composite.

3. Results and discussion

3.1. Fesem

The surface morphology of the PANI-Ag composite is investigated using scanning electron microscope (SEM). As shown in **Fig. 1**a, the PANI layer was formed on the surface of the Ag particle. The elemental analysis (EDX) spectra for PANI/Ag composite is shown in **Fgiure. 1**b. These spectra indicates the

presence of carbon (C), Oxygen (O), Ag atoms as the major components present in the PANI/Ag composite synthesized by in-situ polymerization method.

Surface morphology images of neat and coated PS membranes are shown in **Fig. 2**. SEM results indicates formation of uniform fibers of diameter around 2-3 pm. The images of the coated membranes show formation of uniform coating surrounding the PS fibers. The image of higher magnification indicates formation of PANI nanofibril network. The average fiber diameter around 100 nm was obtained for PANI. However, between the two-coated PS microfiber samples the density of PANI nanofiber is higher than PANI-Ag nanofiber. The reason may due to higher cohesion between PS molecule and PANI-Ag than with pure PANI. Further evidence about the interaction can be observed in XRD analysis results

3.2. Xrd

X-Ray diffraction analysis of all the polymer membranes shown in **Fig. 3**, are done to investigate the structure and crystallinity. From the plot we can see that diffraction pattern of both pure PS and PANI coated PS have two amorphous characteristic peaks at 20 values of 10° and 20°. However, diffraction pattern of PANI-Ag coated PS membrane as several sharp crystalline peaks due presence of Ag. The diffraction peaks at 20 values 27.91°, 32.32°, 43.7°, 46.7°, 54.9° and 57.67° corresponds to the (210), (122), (200), (231), (142) and (241), crystalline planes of Face- centered cubic structure of Ag according to the JCPDS card no: 04-0783.

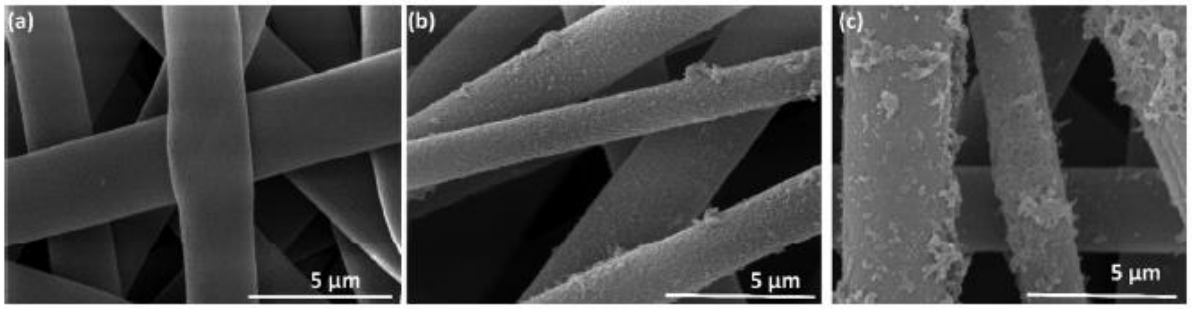

Fig. 2. FESEM images of (a) PS fibers (b) PANI coated PS fibers (c) PANI-Ag coated PS fibers.

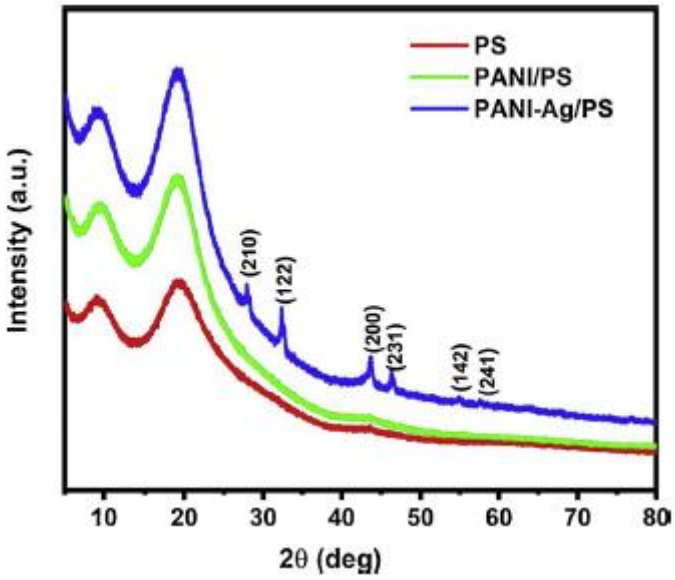

Fig. 3. XRD diffractogram of neat PS membrane, PANI and PANI-Ag coated PS membrane.

3.3. DSC analysis

DSC analysis of all the polymer samples are carried out to understand the glass transition (T_g) under N_2 atmosphere from 30 °C to 250 °C at the heating rate of 10 °C/min. The analysis is done in three cycles. The 1st cycle is heating from 30 °C to 100 °C, second cycle cooling from 100 °C to 30 °C and the final one is heating again from 30 °C to 250 °C.

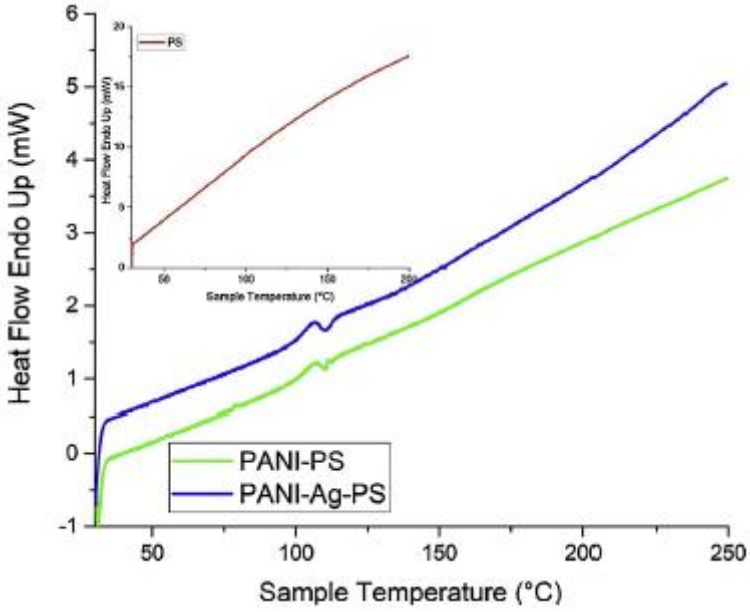

Fig. 4. DSC of PANI-PS and PANI-Ag-PS membrane; inset DSC of pure PS.

Here in **Fig. 4** we only present the results of third heating cycle. The T_g of PANI can be calculated from the DSC curve at the point where sudden slope changes occur. From the figure, T_g is observed for the composite in the temperature range from 100 —110 °C. It is noteworthy that the maximum of the T_g

peak shifted to higher temperature for the PANI-Ag /Ps composite. From DSC thermogram we can also know about physical change such as loss moisture and other solvent used in preparation and chemical change such as decomposition. The evaporation of water and solvents has happened in the 1st heating cycle of analysis.

3.4. TGA analysis

TGA is carried out under N_2 atmosphere from room temperature to 800 °C at the heating rate of 10 °Cmin $^{-1}$ and the results are shown in **Fig. 5**. From the TGA thermogram we observe that pure PS has sharp 100 % degradation in single step and the peak degradation temperature is 416 °C with no residue left behind. However, the coated samples have two steps of gradual degradation process.

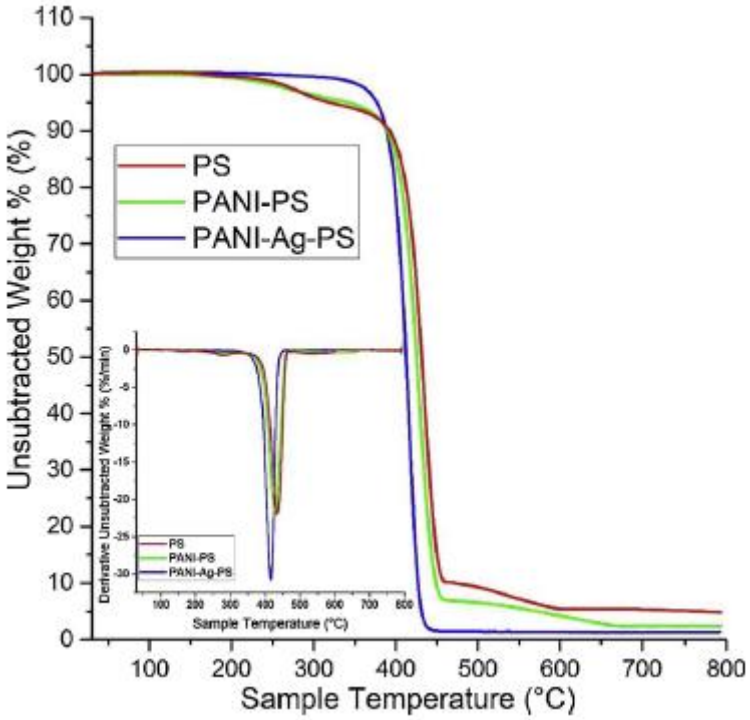

Fig. 5. TGA thermogram of neat PS, PANI and PANI-Ag coated PS membrane; inset is the derivatives of neat PS, PANI and PANI-Ag coated PS membrane.

The 1st step of thermal degradation of PANI and PANI-Ag coated membrane has been soon started with the rise of temperature and completed at around 100 °C. The constitute only 5 % of weight loss and this may be due to evaporation of water and solvents used during synthesis process. The 2nd and final step of both the samples starts around 200 °C and completed at 426 °C for PANI and at 436 °C for PANI-Ag coated sample. After 800 °C PANI-Ag-PSA coated samples is left with 5 % residue, which may be due to presence of Ag in the composite.

3.5. Antimicrobial results

Two bacterial strains were used for evaluation of antibacterial properties, namely Staphylococcus aureus CCM 4516 (inoculum concentration 1.8 x 106 cfu / ml) and Escherichia coli CCM 4517 (inoculum

concentration 0.5 x 106 cfu / ml). The reason was to perform tests on both Gram positive (Staphylococcus aureus) and Gram negative (Escherichia coli) bacterial strains.

Obtained results are listed in the table S1The antibacterial properties are proportional to obtained MIC value. In general, the lower MIC value is obtained, the better antibacterial properties are achieved. The results indicate, that PANI sample do not exhibit any antibacterial performance, when for both Staphylococcus aureus and Escherichia coli reached value > 16mg/ml. However, opposite behavior was observed for PANI Ag sample when antibacterial performance was exhibited. In case of Staphylococcus aureus the MIC reached value of 4 mg/ml. For Gram negative Escherichia coli the result reached 0.5mg/ml what denotes stronger antibacterial effect against Gram negative than Gram positive bacterial strains.

3.6. Photocatalytic aktivity

The photocatalytic degradation of AZG dye in presence of PS/PANI-Ag nanocomposite was studied by using UV-vis spectrophotometer. **Fig. 6**(a, b) shows the degradation of AZG dye under UV light irradiation. The absorption spectra of AZG dye solution in the presence of PS/ PANI-Ag as a function of time is shown in **Fig. 6**a. It is clearly seen that more than 85 % of AZG can be degraded within 180 min. The inset in Fig.1a shows the decolorization of AZG solution. The degradation efficiency is shown in **Fig. 6**b. When the time increases, the percentage removal of dye also increases for the PS/PANI-Ag nanocomposites. The reaction was also carried out for without catalyst and only 4.5 % degradation was achieved in 180 min. The results indicate that the PS/ PANI-Ag nanocompoistes play an important role in AZG degradation process and no degradation was achieved without catalyst. To understand the progress of the reaction and identify the intermediate species formed during the degradation process, we have performed LC-MS analysis for the Azocarmine G dye and the degradation process is shown in Figure (S2-S4). The chemical formula, molar mass and structure of the product is shown in Table S2. LC-MS is recorded for the sample degraded at time interval of 180 min. From the Table S2, the obtained molecular mass and fragment's structure undoubtedly confirms that the inclusion of photoactive polystyrene/(PANI-Ag) in azocarmine dye enhances the photocatalytic degradation and thus photocatalytic activity.

In order to confirm the stability of the nanocomposites, FTIR analysis was performed for PS/PANI-Ag nanocomposites before and after photocatalytic reaction. From the **Fig. 7**, the structural property of the nanocomposite was similar before and after the photocatalytic reaction, which implies that the structure of the PS/PANI-Ag nanocomposite was not affected and also it was not chemically transformed to other organic compounds during the photodegradation process.

3.6.1. Photodegradation mechanism

The photocatalytic mechanism of the PS/PANI-Ag system is shown in **Fig. 8**. In this system PS has been chosen for anchoring PANI-Ag particles.

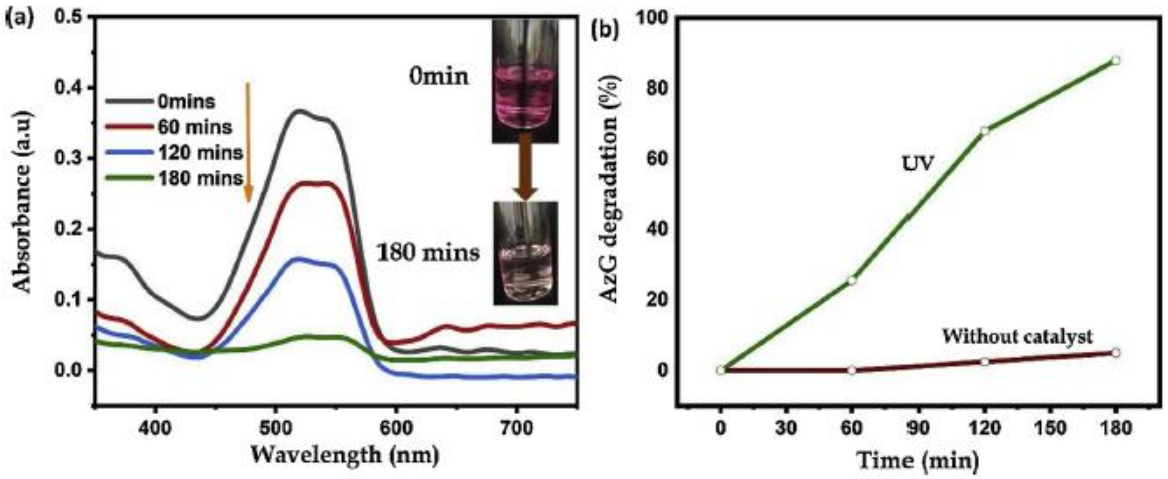

Fig. 6. (a, b) Photocatalytic activity of PS/PANI-Ag system under UV light irradiation. (b) Percentage degradation of AZG dye at different time intervals.

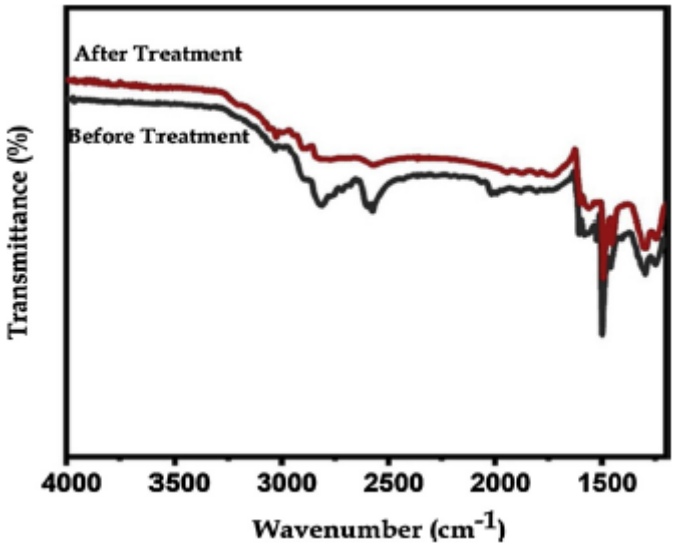

Fig. 7. FTIR spectra of PS/PANI-Ag nanocomposite before and after UV light irradiation.

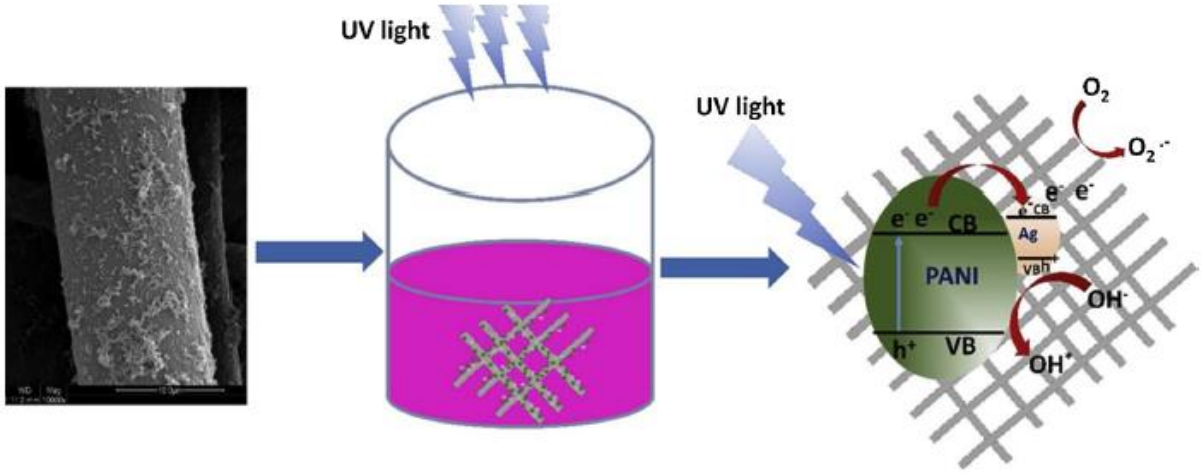

Fig. 8. Photocatalytic degradation mechanism.

When a photon of energy falls on the PS/PANI-Ag nanocomposite catalytic surface, the electron-hole pairs are generated. These charge carriers act as photocatalytic active center [**26**]. Due to the fact that PANI can absorb light to induce $\pi - \pi^*$ transition, delivering the excited state electrons of the highest occupied molecular orbital (HOMO) to the lowest unoccupied molecular orbital (LUMO) [**27**]. PANI is strongly excited and produce photogenerated electrons on the LUMO of PANI. The excited electrons from the conduction band of PANI are transferred to the conduction band of Ag. Which stimulated oxygen to give superoxide radicals ion O_2^{*-} and similarly the holes generated in the valence band react with water molecules to form hydroxyl radicals (*OH). These hydroxyl and superoxide radicals are the powerful tool to degrade the organic pollutant [**28,29**], equation [**1-6**].

$$PANI + h\nu \rightarrow PANI + (e + h) \quad (1)$$

$$PANI\,(e) + Ag \rightarrow PANI + Ag\,(e) \quad (2)$$

$$Ag\,(e) + O_2 \rightarrow O_2^{*} - + Ag\,(h) \quad (3)$$

$$Ag\,(h) + PANI \rightarrow PANI\,(h) \quad (4)$$

$$PANI\,(h) + OH^{-} \rightarrow PANI + {}^*OH \quad (5)$$

$$PANI\,(h) + {}^*OH + O_2^{*} - + AZG \rightarrow H_2O + CO_2 \quad (6)$$

4. Conclusion

PANI-Ag nanocomposite coated PS membrane with ability of strong photocatalytic degradation ability and antimicrobial property is successfully prepared and studies. Antimicrobial study performed using pure PANI sample does not show any antibacterial performance for both Staphylococcus aureus and Escherichia coli. Whereas, reverse behavior is observed for PANI-Ag samples. In case of Staphylococcus aureus the MIC reached value of 4 mg/ml and for Gram negative Escherichia coli the result reached 0.5mg/ml. This result indicates stronger antibacterial effect against Gram negative than Gram positive bacterial strains. The photocatalytic degradation performance of the PANI-Ag on PS membrane shows 85 % removal of AZO dye from the solution in a span of 180 mints without any change in chemical composition of the membrane.

References

[1] K.A. Adegoke, O.S. Bello, Dye sequestration using agricultural wastes as adsorbents, Water Resour. Ind. 12 (2015) 8-24, https://doi.org/10.1016/j.wri.2015.09.002.

[2] S.A. Da Franęa, M.F. Dario, V.B. Esteves, A.R. Baby, M.V. Velasco, Types ofhair dye and their mechanisms of action, Cosmetics 2 (2) (2015) 110-126, https://doi.org/ 10.3390/cosmetics2020110.

[3] A. Hagfeldt, U.B. Cappel, G. Boschloo, L. Sun, L. Kloo, H. Pettersson, E.A. Gibson, Dye-sensitized photoelectrochemical cells, Practical Handbook of Photovoltaics, Elsevier, 2012, pp. 479-542, https://doi.org/10.1016/B978-0-12-385934-1. 00015-5.

[4] R. Kant, Textile dyeing industry an environmental hazard, Nat sci. 4 (2011) 5, https://doi.org/10.4236/ns.2012.41004.

[5] F. Kebede, A. Gashaw, Removal of chromium and azo metal-complex dyes using activated carbon synthesized from tannery wastes, Open Access J. Sci. Technol. 5 (2017) 30, https://doi.org/10.11131/2017/101214.

[6] S. Lacorte, A. Latorre, D. Barcelo, A. Rigol, A. Malmqvist, T. Welander, Organic compounds in paper-mill process waters and effluents, Trac Trends Anal. Chem. 22 (2003) 725-737, https://doi.org/10.1016/S0165-9936(03)01009-4.

[7] M. Šuleková, M. Smrvova, A. Hudak, M. Hezelova, M. Fedorova, Organic colouring agents in the pharmaceutical industry, Folia Vet. 61 (3) (2017) 32-46, https://doi. org/10.1515/fv-2017-0025.

[8] T.O. Durotoye, A.A. Adeyemi, D.O. Omole, O. Nakunle, A. Ahsan, Impact assessment of wastewater discharge from a textile industry in Lagos, Nigeria. Cogent Eng. 5 (2018) 1531687, , https://doi.org/10.1080/23311916.2018.1531687.

[9] N. Azbar, T. Yonar, K. Kestioglu, Comparison of various advanced oxidation processes and chemical treatment methods for COD and color removal from a polyester and acetate fiber dyeing effluent, Chemosphere. 55 (1) (2004) 35-43, https://doi. org/10.1016/j.chemosphere.2003.10.046.

[10] P. Cunico, A. Kumar, R. Alcantara, D.A. Fungaro, Adsorption of solophenyl dyes from aqueous solution by modified nanozeolite from bottom ash and its toxicity to C. Dubia, Curr. Nanomater. 2 (2) (2017) 95-103, https://doi.org/10.2174/ 2405461503666180201152351.

[11] J. Forss, M.V. Lindh, J. Pinhassi, U. Welander, Microbial biotreatment of actual textile wastewater in a continuous sequential rice husk biofilter and the microbial community involved, PLoS One 12 (2017) e0170562, , https://doi.org/10.1371/ journal.pone.0170562.

[12] R. Lafi, L. Gazara, R.H. Lajimi, A. Hafiane, Treatment of textile wastewater by a hybrid ultrafiltration/electrodialysis process, Chem. Eng- Process. Intens. 132 (2018) 105-113, https://doi.org/10.1016Z.cep.2018.08.010.

[13] E.M. Saggioro, A.S. Oliveira, J.C. Moreira, Heterogeneous photocatalysis remediation of wastewater polluted by indigoid dyes, Tex. Waste. Treat. 93 (2016), https:// doi.org/10.5772/63790.

[14] M. Zielińska, M. Galik, Use of ceramic membranes in a membrane filtration supported by coagulation for the treatment of dairy wastewater, Water Air Soil Pollut. 228 (2017) 173, https://doi.org/10.1007/s11270-017-3365-x.

[15] U.S.P. Uday, T.K. Bandyopadhyay, B. Bhunia, Bioremediation and detoxification technology for treatment of dye (s) from textile effluent, Textile Wastewater Treatment; Croatia, Intechopen (2016) 75-92, https://doi.org/10.5772/62309.

[16] S. Gligorovski, R. Strekowski, S. Barbati, D. Vione, Environmental implications of hydroxyl radicals (• OH), Chem. Rev. 115 (2015) 13051-13092, https://doi.org/10. 1021/cr500310b.

[17] H. Kaur, G. Hippargi, G.R. Pophali, A.K. Baniwal, Treatment methods for removal of pharmaceuticals and personal care products from domestic wastewater, Pharmaceuticals and

Personal Care Products, Waste Management and Treatment Technology, Elsevier, 2019, pp. 129-150, https://doi.org/10.1016/B978-0-12-816189-0.00006-8.

[18] Z.S. Seddigi, S.A. Ahmed, S.P. Ansari, N.H. Yarkandi, E. Danish, M.D. Oteef, A.M. Abulkibash, Photocatalytic degradation of methyl tert-butyl ether (MTBE): a review, Adv. Environ. Res. 3 (2014) 11-28, https://doi.org/10.12989/aer.2014.3. 1.011.

[19] Q. Ding, Y.-E. Miao, T. Liu, Morphology and photocatalytic property of hierarchical polyimide/ZnO fibers prepared via a direct ion-exchange process, ACS appl. mat & int. 5 (12) (2013) 5617-5622, https://doi.org/10.1021/am4009488.

[20] E.T. Soares, M.A. Lansarin, C.C. Moro, A study of process variables for the photocatalytic degradation of rhodamine B, Brazilian J. Chem. Eng. 24 (1) (2007) 29-36, https://doi.org/10.1590/S0104-66322007000100003.

[21] M.M. Mahlambi, C.J. Ngila, B.B. Mamba, Recent developments in environmental photocatalytic degradation of organic pollutants: the case of titanium dioxide na-noparticles—a review, J. Nanomaterials 5 (2015), https://doi.org/10.1155/2015/ 790173.

[22] S.L. Lee, C.J. Chang, Recent developments about conductive polymer based composite photocatalysts, Polymers. 11 (2) (2019) 206, https://doi.org/10.3390/ polym11020206.

[23] V. Najafi, E. Ahmadi, F. Ziaee, H. Omidian, H. Sedaghat, 2 Polyaniline-Modified TiO, A highly effective photo-catalyst for solid-phase photocatalytic degradation of PVC, J. Poly. Environ. 27 (4) (2019) 784-793, https://doi.org/10.1007/s10924-018-01363-1.

[24] R. Tanwar, U.K. Mandal, Photocatalytic activity ofNi 0.5 Zn 0.5 Fe 2 O 4@ polyaniline decorated BiOCl for azo dye degradation under visible light-integrated role and degradation kinetics interpretation, RSC Adv. 9 (16) (2019) 8977-8993, https://doi.org/10.1039/C9RA00548J.

[25] Y. Bu, Z. Chen, Role of polyaniline on the photocatalytic degradation and stability performance of the polyaniline/silver/silver phosphate composite under visible light, ACS app. mat. & int. 6 (20) (2014) 17589-17598, https://doi.org/10.1021/ am503578s.

[26] S. Wang, D. Li, C. Sun, S. Yang, Y. Guan, H. He, Synthesis and characterization of g-C3N4/Ag3VO4 composites with significantly enhanced visible-light photocatalytic activity for triphenylmethane dye degradation, Appl. Catal. B: Environ. 144 (2014) 885-892.

[27] L. Zhang, M. Wan, Polyaniline/TiO2 composite nanotubes, J. Phy. Chem B. 107 (28) (2003) 6748-6753, https://doi.org/10.1021/jp0341130g.

[28] S. Yang, X. Cui, J. Gong, Y. Deng, Synthesis of TiO 2-polyaniline core-shell nanofibers and their unique UV photoresponse based on different photoconductive mechanisms in oxygen and non-oxygen environments, Chem Comm. 49 (41) (2013) 4676-4678, https://doi.org/10.1039/C3CC39157D.

[29] Z. Zhao, Y. Zhou, W. Wan, F. Wang, Q. Zhang, Y. Lin, Nanoporous TiO2/polyaniline composite films with enhanced photoelectrochemical properties, Mate Letters. 130 (2014) 150-153, https://doi.org/10.1016Z.matlet.2014.05.099.